Journal of Materials Chemistry B

Accepted Manuscript

ROYAL SOCIETY OF CHEMISTRY

www.rsc.org/materialsB

Journal Name Journal of Materials Chemistry B Dynamic Article Links►

Cite this: DOI: 10.1039/c0xx00000x

www.rsc.org/xxxxxx

ARTICLE TYPE

Enhanced loading and controlled release of rhBMP-2 in thin mineralized collagen coatings by aid of chitosan nanospheres and its biological evaluations

ZiqiangKong[1], Jun Lin[1], Mengfei Yu[1], LanYu, Juan Li, WenjianWeng*, KuiCheng*, HuimingWang*

Received (in XXX, XXX) XthXXXXXXXXX 20XX, Accepted Xth XXXXXXXXX 20XX
DOI: 10.1039/b000000x

Loading of an appropriate amount of rhBMP-2 and avoiding its "burst-release" are key challenges for upgrading the biological performance of thin bioactive coatings on metal implants. In this study, we adopted incorporation of chitosan nanospheres into thin mineralized collagen coatings to enhance rhBMP-2 loading and improve releasing behavior based on the good affinity of chitosan for proteins and the large surface area of nanospheres. We realized the incorporation process by electrophoretic injection. Using chitosan nanospheres, we were able to increase the rhBMP-2 loading amount in the thin coating by 2.7-fold (from 446 ng/cm^2 to 1186 ng/cm^2), and showed that the rhBMP-2 exhibited sustained release behavior. MC3T3-E1 cells cultured on the rhBMP-2/chitosan nanosphere-incorporated thin coatings (Col/Cs/BMP) showed good cell attachment and proliferative behavior, and high levels of differentiation and mineralization. In *in vivo* tests, spiral CT analysis and histological observations demonstrated that Col/Cs/BMP coatings on metal implants were able to increase bone density and accelerate new bone growth after implantation for 4 and 8 weeks, the boundary between host bone and new bone disappeared after implantation for 8 weeks. The pull-out tests further confirmed that the Col/Cs/BMP coatings could significantly enhance osseointegration. The present results indicate that incorporation of chitosan nanospheres into thin coatings is an effective way to enhance the loading amount properly, improve the release behavior of rhBMP-2 and finally accelerate the osseointegration process.

* Corresponding author. Tel. and Fax : +86 571 87953787
Email address: wengwj@zju.edu.cn, chengkui@zju.edu.cn, wangmysm@yahoo.com.cn
[1] Contributed equally.

Cite this: DOI: 10.1039/c0xx00000x

www.rsc.org/xxxxxx

ARTICLE TYPE

1 Introduction

Metal implants are indispensible in orthopedic surgeries as metal devices are able to bear mechanical loads and to provide stabilization so that optimal alignment and function of bone can be maintained following substitution of bones and joints[1]. However, medical metals usually have poor biocompatibility, low rates of osseointegration and require a long period of postoperative recovery.

Advanced strategies focus on the anchorage of bioactive coatings to the metal surface and on the delivery of osteogenic signaling molecules to enhance peri-implant bone regeneration[2]. Biologically active components are immobilized onto the metal implant surface through a variety of procedures such as adsorption, covalent coupling, electrochemical surface modifications and self organized organic layers[3-5]. These surface modifications can promote cell attachment, proliferation and differentiation, thus accelerating the growth of bone tissue at bone-implant interfaces[6].

Among osteogenic signaling molecules, bone morphogenetic protein (BMP) family members are considered to be the best due to their highly osteogenic ability[7]. Previous reports have demonstrated that BMP-2 can stimulate the proliferation, migration and osteogenic differentiation of mesenchymal stem cells[8, 9]. Moreover, BMP-2 has been proven to induce osteogenesis *in vivo*[10, 11]. Although BMPs are potent osteoinductive growth factors, their administration for orthopedic applications is complicated by their short biological half-lives, localized actions and rapid local clearance[12]. Effective BMP treatment of bone defects requires their incorporation into biomaterials for locally sustained delivery at the target site[13].

Incorporation of BMPs into the thin coatings used on implants necessitates overcoming two difficulties: limitation of the loading amount and prevention of burst-release behavior. Recent studies of thin coatings using BMP-2 loaded at 200–300 ng/cm^2 [4]found that 80% of the incorporated BMP had already been exhausted after the first week of release[14], which may prolong the osseointegration period *in vivo*. These challenges have been addressed using many porous thin bioactive coatings[4, 14, 15].

We previously showed that mineralized collagen coatings on titanium implants have good cytocompatibility[16, 17]. However, the composition of mineralized collagen shows low affinity with rhBMP-2[18], and the porous structure of a mineralized collagen coating is not suitable for effective loading of rhBMP-2 nor for sustained release behavior.

Chitosan is cationic [19] and has rich side groups (-NH_2, -OH) that can be bonded to drug molecules and growth factor proteins; it is wildly utilized as a carrier for drugs [20] and proteins such as BMPs[21, 22]. In this study, we employed chitosan as a binding agent to hold BMP-2 to enhance its loading/releasing performances in mineralized collagen coatings. The chitosan nanospheres and BMP-2 were simultaneously incorporated into mineralized collagen coatings by electrophoretic injection. The presence of chitosan nanospheres in mineralized collagen coatings can reduce their porosity and increase their tortuosity[17], and the resulting microstructural changes are greatly beneficial for sustained release of BMP-2.

In this study, the primary purpose is to enhance the loading amount of rhBMP-2 to a proper amount, and the second purpose is to prolong the release period of rhBMP-2. After realizing the two purposes, the osseointegration process is hoped to be accelerated to a desirable degree.

The microstructure of the rhBMP-2/chitosan nanosphere-incorporated thin coatings (Col/Cs/BMP) was characterized, and the loading amount and release profile of rhBMP-2 were measured. The cytological compatibility of the Col/Cs/BMP coatings was evaluated by assessing the proliferation, migration and osteogenic differentiation of mesenchymal stem cells cultured on the coatings. Finally, the osseointegration effect was assessed by spiral CT analysis, histological observations and pull-out tests of coated titanium rods implanted into New Zealand white rabbits.

2 Materials and Methods

2.1 Preparation of different coatings

2.1.1 Preparation of mineralized collagen coatings

To prepare electrolytic solutions, type I collagen (Beijing

Yierkang Co., Beijing, China) was dissolved in 5 mM acetic acid to a final concentration of 0.5 mg/mL, and then stored at 4°C. $Ca(NO_3)_2$ and $NH_4H_2PO_4$ were dissolved in distilled water and soluble type I collagen was added to the electrolyte to final concentrations of 4 mM Ca^{2+}, 8 mM PO_4^{3-}, and 0.4 mg/mL collagen. An NaOH solution (0.25 M) was used to adjust the pH of the electrolyte to 4.5 with a calibrated pH meter (Thermo, Benerly, MA). Titanium plates or rods (Bangnuo Co. Baoji, China) (99.9% Ti, Medical grade) were cleaned ultrasonically in ethanol, and acid-etched by a mixed acid solution composed of 2.75 M HF and 3.94 M HNO_3.

Electrochemically-assisted deposition[16] was carried out in a two-electrode electrochemistry system, involving a Ti plate (rod) as the working electrode, i.e. the cathode, and a platinum plate (15 × 25 × 0.1 mm^3) or a rod (3.0 mm in diameter) as the anode. The distance between the anode and the cathode was fixed at 15 mm. During the deposition, the electrochemical cell with the electrolyte mixture was kept at 37°C and a constant potential (2.1 V) was applied.

After 30 minutes deposition, a mineralized collagen coating (referred to as Col) formed on the Ti cathode. The coated Ti was then dried in an oven at a temperature of 37°C.

2.1.2 Preparation of rhBMP-2/chitosan nanosphere solutions

The chitosan (degree of deacetylation: 95%, Shandong Aokang Co.) was dissolved in 166.7 mM acetic acid to a final concentration of 12.5 mg/mL. Tri-polyphosphate (TPP) (WuXiXiniu Co.) was dissolved in deionized water to a concentration of 12.5 mg/mL. Human recombinant BMP-2 (Shanghai Rebone Biomaterials Co.) was dissolved in distilled water and chitosan (final concentration: 0.12 mg/mL) was added to the solution, then the mixed solution was flush mixed with the TPP solution (final concentration: 0.08 mg/mL). The chitosan-TPP-rhBMP-2 nanospheres started to form spontaneously via a TPP-initiated ionic gelation mechanism. The final concentration of rhBMP-2 was 2 μg/mL. An NaOH solution (0.25 M) was used to adjust the pH of the mixed solution (nanospheres with rhBMP-2) to 7, and the mixed solution (S1) was then stirred for 24 h at room temperature.

Another rhBMP-2 solution (S2; without chitosan nanospheres) was prepared at a concentration of 2 μg/mL. Acetic acid (0.25 M) was used to adjust the pH to 7.

2.1.3 Preparation of rhBMP-2/chitosan nanosphere-incorporated coatings

After the coatings on the Ti plates were completely dried, they were put into the S1 or S2 solution as the electrolytic cathode for 3 h. The solutions were kept at 37°C under a constant potential of 1V. In this electric field, the rhBMP-2 moved into the mineralized collagen coating (referred to as Col/BMP) in the S2 solution. In the S1 solution, chitosan nanospheres with rhBMP-2 were electrophoretically injected into the coating (referred to as Col/Cs/BMP). The uncoated titanium was referred to as Ti (blank control).

2.2 Measurements of rhBMP-2 loading amount and release

To measure rhBMP-2 loading amount, the S1 and S2 solutions were centrifuged after the electrochemical process, and the supernatant was collected. The rhBMP-2 concentration in the supernatant was measured with a BMP-2 Quantikine ELISA Kit(Shanghai Yanjin Co), and the amount of rhBMP-2 loaded on the coatings could then be calculated from the initial rhBMP-2 amount and the amount remaining in the supernatant.

rhBMP-2 release from the BMP-loaded coatings was analyzed by immersion in 5 mL phosphate-buffered saline (PBS), and the amount of rhBMP-2 released was also measured with a BMP-2 Quantikine ELISA Kit. The release profiles of each experimental set were expressed by plotting the released amount/percentage vs. time.

2.3 Kinetic analysis of the release behavior

The release process from thin coatings is commonly divided into two stages[17]: burst release (from the proximal surface of the coatings) and sustained release (from the interior of the coatings). Here, an empirical equation, $Q = kt^{1/2}+b$, is adopted to evaluate the burst release degree, where Q is the release amount after time t per unit exposed area, k represents the release rate, and b is a constant which represents the possibility of a burst release [23].

2.4 Characterization of coatings

The morphologies and microstructures of the resulting coatings were characterized by scanning electron microscopy (FE-SEM Hitachi, SU-70, S-4800), and the phase of the coatings was measured by XRD (X' Pert PRO, Cu Ka, 0.02 per step).

2.5 Cell culture and seeding

Mouse calvaria-derived, pre-osteoblastic cells (MC3T3-E1, CRL-2594, ATCC) were used in this study. MC3T3-E1 cells were

cultured on titanium with different coatings (Ti, Col, Col/BMP, Col/Cs/BMP) in alpha-modified Minimum Essential Medium (MEM Alpha, Gibco) supplemented with 10% fetal bovine serum (FBS, PAA, Australia), 1% sodium pyruvate, 1% antibiotic solution containing 10,000 units/mL penicillin and 10,000 μg/mL streptomycin, and 1% MEM non-essential amino acids (all from Gibco) under a humidified atmosphere of 5.0% CO_2 at 37°C. Subconfluent MC3T3-E1 cells growing on tissue culture polystyrene (TCPS) were trypsinized with 0.25% trypsin, 1 mM EDTA (Gibco), and were subcultured on different coatings.

Initial proliferation of MC3T3-E1 on titanium surfaces was evaluated by measuring the number of cells attached to titanium substrates after incubating for 6 and 24 h. Propagated cells were quantified in terms of cell density at 2 and 5 days of culture. A cell suspension (500 μL) with a density of 5×10^4 cells/cm^2 was inoculated into a 24-multiwell plate containing the samples with different surfaces. After 6 and 24 h, samples were transferred to another 24-well plate after washing 3 times with PBS. Cell proliferation rate was evaluated using cell counting kit-8 (CCK-8, Dojindo Laboratories, Kumamoto, Japan). The absorbance was measured on a microplate reader at a wavelength of 450 nm.

2.6 Cell morphological observations

To evaluate the initial attachment behaviors of cells on coatings, MC3T3-E1 cell morphology was observed by SEM. After 3 h, the culture medium was removed and the specimens were fixed with 2.5% glutaraldehyde in PBS overnight at 4°C. After dehydration in graded alcohols, the specimens were dried using hexamethyldisilazane (HMDS, Sigma-Aldrich, St Louis, MO). They were then sputter-coated with gold. The surface of the specimen was finally examined with secondary electrons by SEM at a voltage of 15 kV.

Confocal laser scanning microscopy (CLSM) was used to examine cell morphology and cytoskeletal arrangement in pre-osteoblasts seeded onto various titanium surfaces. After 3 h of culture, cells were fixed in 10% formalin and stained with goat anti-actin polyclonal antibody (SC-1615, Santa Cruz Biotechnology, Santa Cruz, CA), followed by a Dylight™ 594-conjugated anti-goat secondary antibody (Jackson). Cultures were also immunochemically stained with mouse anti-vinculin monoclonal antibody (Abcam, Cambridge, MA), followed by a FITC-conjugated anti-mouse secondary antibody (Abcam) and counterstained with 10 μg/mL Hoechst 33258 (Sigma-Aldrich) at room temperature for 5 min. The cell morphology and cytoskeletal arrangement were quantified using image analysis software (Image J, NIH, Bethesda, ML).

2.7 Alkaline phosphatase (ALP) assay

To determine the osteogenic activity of the mouse MC3T3-E1 cells, ALP activity was assayed colorimetrically. Mouse MC3T3-E1 cells were cultured on different surfaces for 7 and 14 days. At the end of the culture period, the cells were rinsed with PBS, vigorously lysed in PBS containing 0.2% Triton X-100 for 10 min, and then centrifuged. After centrifugation, the supernatant was used to determine the total intracellular protein and ALP activity with ρ-nitrophenyl phosphate as the substrate. The absorbance at 405 nm was measured with a spectrophotometric microplate reader (Bio-Rad 680, USA). The ALP activity was normalized to total intracellular protein synthesis and thus expressed as μmol ρ-nitrophenol/min/mg protein. The total intracellular protein content was determined with a BCA kit.

2.8 Quantitative real-time PCR

MC3T3-E1 cells grown on different surfaces were collected after culture for 7 and 14 days. Total RNA was extracted from cultured MC3T3-E1 cells grown on titanium (1 × 1 cm^2) with different coatings using the TRIzol reagent (Invitrogen, San Diego, CA) according to the manufacturer's recommended protocol. Real-time PCR was performed in a Light Cycler using SYBR green detection for expression of type I collagen and osteocalcin mRNA. Gene expression was normalized to the housekeeping gene GAPDH. The results were analyzed by the 2-ΔΔCT method.

2.9 Quantification of mineralization

MC3T3-E1 cells cultured on different surfaces (n = 3) were stained with alizarin red S after culture for 21 days, according to a previously described method[4, 24]. Briefly, the cells were fixed with cold methanol for 10 min and washed with deionized water prior to immersion for 3 min in 370 μL of 1% Alizarin Red S (Sigma) solution dissolved in a 1:100 (v/v) ammonium hydroxide/water mixture. Each stained specimen was washed several times with deionized water and air-dried at room temperature. The stained specimen was photographed to show the amount of calcium deposition. Bone nodule formation[25] of the cells cultured on the different surfaces on day 21 of cell culture was observed by SEM, and the presence of calcium on the cell-

cultured specimens was characterized by energy dispersive X-ray spectroscopy (EDX) mapping.

2.10 Animals and surgical procedure

The animal protocol was approved by the Ethics Committee for Animal Research, Zhejiang University, China. The rod samples (ø 3 mm × 8 mm) with different coatings (Ti, Col, Col/BMP, Col/Cs/BMP) were implanted into the femoral metaphyses of mature New Zealand White rabbits with an average weight of 2.5–3 kg to evaluate the osteogenic effect of the different surfaces (n = 20 per group). After anesthesia, the surgical areas of the rabbits were shaved and disinfected, and a skin incision of approximately 3 cm was created to expose the femoral epiphysis. A cylindrical hole (3.1 mm in diameter) was created in the femoral epiphysis using a surgical drill 13 mm in length, and the test rods were inserted into the predrilled holes. Finally, the soft tissue layers and skin were closed with absorbable sutures and the surgical site was disinfected again. Postoperatively, benzyl penicillin (40,000 U/kg) was administered intramuscularly daily for 3 days. The animals were sacrificed under general anesthesia after 4 and 8 weeks, and the femoral condyles containing the implants were fixed in 4% paraformaldehyde for 48 h.

2.11 Spiral computed tomography analysis (Spiral CT)

CT values were used to analyze the effect of bone mineral density around the implant. After sacrifice, the femoral condyle samples containing implants were scanned with 64-slice spiral CT (Philips Brilliance, Philips, Germany). The data were measured and assessed using the standard CT software "Dicom Works". The ROI (region of interest) was restricted to a 0.5 mm area surrounding the implant. The CT values in the ROI were analyzed to reflect the bone mineral density. The resolution of CT images was 0.33 mm.

2.12 Histological analysis

After fixation in paraformaldehyde, the samples were divided into two groups. Forty specimens were soaked in 10% ethylenediamine tetra-acetic acid (EDTA) for decalcification. The remaining specimens were preserved in 70% ethanol for pull-out testing. After decalcification, the samples were cut in half longitudinally along the long axis of the implant, then the implants were gently removed. The tissues were dehydrated, cleared and embedded in paraffin. Tissue sections, approximately 6 mm in thickness, were mounted on glass slides and stained with hematoxylin and eosin (H&E). The slices were examined under a light microscope (Olympus, Tokyo, Japan).

2.13 Pull-out testing

A tensile pull-out test was performed to evaluate the bone-to-implant strength. Bone specimens were kept in 70% ethanol in the way to mechanical test on the same day to minimize the influences that external environment brought. The femora were carefully prepared in order to fit into a custom jig. Specimens were tested at a loading rate of 1 mm/min with a 20 KN load cell in a universal testing machine (CMT 4000, displacement resolution 0.03 μm, MTS-SANS company). The peak power is the maximum load value that represents the biomechanical bone strength. The level of significance was set at $P< 0.05$.

2.14 Statistical analysis

All values are expressed as means ± standard deviation. Statistical analyses were carried out by one-way analysis of variance (one-way ANOVA) and Scheffe's post hoc test using SPSS software for multiple comparison tests, or using Student's t-test. Differences were considered statistically significant when $P< 0.05$.

3. Results

3.1 Characterization of the coatings

3.1.1 Microstructure of the coatings

The as-prepared mineralized collagen coating was porous in morphologyand approximately 40–50 μm in thickness (Fig 1a and Fig.1a-1). After electrophoretic injection, chitosan nanospheresweare incorporated into the pores of the mineralized collagen coating (Fig. 1b), and the morphology and thickness of the resulting coating were not markedly changed (Fig. 1b and Fig. 1b-1). The XRD patterns shown in Fig. 2 indicate that both the rhBMP-2 loaded coatings (Col/BMP, Col/Cs/BMP) contained hydroxyapatite (HA, JCPDS 09-0432) phases.

3.1.2 *In vitro* rhBMP-2 loading/release profile of the different coatings

As shown in Fig. 3, the loading amount of rhBMP-2 in the Col/BMP coating was approximately 446 ng/cm^2, but in the Col/Cs/BMP coating it increased 2.7-fold to reach 1,186 ng/cm^{2}with the addition of chitosan nanospheres. After soaking for 11 days, approximately 58.5% of the rhBMP-2 had been released from the Col/BMP coating, while only 39.5% was released from the Col/Cs/BMP coating, demonstrating that this coating showed sustained release behavior (Fig. 4).

3.1.3 Kinetic analysis

The Q-$t^{1/2}$ curves and the linear fits of curves of rhBMP-2

release from different coatings are shown in Fig. 5. The two stages could make sense in understanding the release behavior because BMP loading in a thin coating has a limited interior BMP existence. During the first release stage, parameter b [17, 23] was related to the initial amount of rhBMP-2 released. In comparison with coatings without chitosan nanospheres, the intercept b (shown in linear fit 1) decreased from 0.17 to -10.02, and this reduction indicates that the rhBMP-2 was dispersed more uniformly throughout the coating rather than only being adsorbed on the surface, while the negative value of b indicates depression of the trend for burst release of rhBMP-2. During the second stage, parameter k (shown in linear fit 2) decreased from 12.47 to 8.74 after incorporation of chitosan nanospheres, indicating that the Col/BMP coating had a slower rhBMP-2 release rate and exhibited sustained release behavior. The burst-release depression and release retardation could be attributed to an increase in the affinity of chitosan for rhBMP-2 as well as increased tortuosity of the porous coating due to incorporation of nanospheres[26]. On one hand, the incorporation of chitosan nanospheres increased the affinity of coating and rhBMP-2, and this increased the bonding strength between coating and rhBMP-2, so the difficulty of release from coating for rhBMP-2 also increased. On the other hand, the incorporation of chitosan nanopheres changed the microstructure of the coating : the toutorsity of porous coating increased, directly leading to the changes of diffusion path of rhBMP-2. Both the two reasons lead to the slowing release rate of rhBMP-2.

3.2 *In vitro* cell culture tests

Fig. 6 shows the adhesion and proliferation of cells on the different coatings. Cells were cultured for 6 and 24 h in order to observe differences in cell attachment, and for 3 days and 5 days to observe differences in cell proliferation. When incubated for 6 and 24 h, there were no obvious differences in cell attachment among the different groups. After culture for 3 and 5 days, the OD value of the cells cultured on the coatings increased with rhBMP-2 loading, with the Col/Cs/BMP coating showing the highest OD value. On the whole, the cells on the mineralized collagen coatings with or without rhBMP-2 demonstrated good cell proliferation, although that on the Col/Cs/BMP coating was better.

Intensive and extensive vinculin expression signals appeared within the cytoplasm and around the edges of cells grown on the Col coating (Fig. 7b), and the cells spread well with filopodia embedded into the coating (Fig. 8b and b-1). On Col/BMP and Col/Cs/BMP coatings, vinculin was also well distributed in the cells (Fig. 7c and 7d), with filopodia embedded deeply into the coatings (Fig. 8c-1 and 8d-1), which implies that cell attachment was good. In contrast, only weak vinculin expression (Fig. 7a) and discrete cells with no extended pseudopodia could be observed on the Ti surface (Fig. 8a and 8a-1).

3.2.2 Cell differentiation

As can be seen from Fig. 9, the level of ALP expressed by cells cultured on all coatings increased over the period from 7 to 14 days. The ALP expression level of cells cultured on the Col/Cs/BMP coating for 7 days was significantly higher (by approximately 20%) than that of cells on Col alone and approximately 50% higher than those grown on Ti ($P < 0.01$), and this increase in ALP expression indicates the increased differentiation of cells cultured on the Col/Cs/BMP coating. This increase is thought to play a key role in subsequent osseointegration: ALP reduces phosphate-containing substances (mineralized collagen) to produce the free phosphate required for bone mineralization [27]. However, there were no significant differences among cells cultured on the different coatings for 14 days, which could be attributed to the fact that ALP is an early marker of differentiation, indicating that cells on the Col/Cs/BMP coating differentiated more rapidly but that cells on the other coatings later caught up so that the difference weakened with time.

For the later indicators of differentiation osteocalcin[28] (OC) and collagen I(Col I), the expression of OC in cells cultured on the Col/Cs/BMP coating for 7 and 14 days was higher than that of cells cultured on Col or Col/BMP coatings or Ti control (Fig. 10a). The Col/Cs/BMP coating also resulted in a higher level of expression of Col I than any of the other groups (Fig. 10b)

3.2.3 Cell mineralization

Calcium-rich mineralized nodules appeared in cells cultured on all coatings as well as in controls (Fig. 11), but the number and size of the nodules in cells grown on the Col/Cs/BMP coating was apparently greater than that of any of the other groups. Alizarin red staining (Fig. 11 inset) and EDS mapping (Fig. 11, bottom row) demonstrates that the cells cultured on the Col/Cs/BMP coating exhibited a higher mineralization level and had the highest calcium phosphate content in the extracellular matrix. Analysis of cells on the Col/BMP coating revealed that the addition of rhBMP-2 led to only a small increase in calcium

content from 1.19% (Fig. 11b-1) to 1.42% (Fig. 11c-1). However, the calcium content increased to 2.59% (Fig. 11 d-1) on the Col/Cs/BMP coating, with this significant increase indicating that the Col/Cs/BMP coating has a greater capability to enhance mineralization [29]. In comparison with the Col/BMP group, the increased mineralization (45.17%) of cells on the Col/Cs/BMP coating could help to greatly accelerate the osseointegration process after implantation[30].

3.3 *In vivo* tests

To evaluate the role of different coatings in the growth of bone tissue on implants, spiral CT was employed to characterize bone density around the implant, a parameter which is considered to be key to the assessment of new bone formation after implantation. As shown in Fig. 12, the bone density around the implant increased with time, and the density around the implants with Col, Col/BMP and Col/Cs/BMP coatings was higher than that around Ti implants after 4 and 8 weeks. The density around the Col/Cs/BMP-coated implants at both 4 and 8 weeks after implantation demonstrated significant differences ($P<0.01$ and $P<0.05$) from the Ti group at the same time points. Although the artifacts of implants were present, the results here were only to show the enhancement trend of osseointegration process with the help of chitosan nanospheres.

Hematoxylin and eosin (H&E) staining of decalcified samples was employed to evaluate osteogenesis at the interface between implant and host bone. After implantation for 4 weeks, a mass of fibrous and non-connective tissues could be seen around the implant in the Ti (Fig. 13a-1) and Col groups (Fig. 13b-1), while these tissues were replaced by dense bone matrix (fewer small blue arrows and more small black arrows) in the groups with Col/BMP (Fig. 13c-1) and Col/Cs/BMP-coated implants (Fig. 13 d-1). After implantation for 8 weeks, the density of the bone matrix increased in all groups in comparison with the results at 4 weeks; however, the bone matrix (stained red at the interface) was still sparse in the Ti group (Fig. 13a-2), while connective and compact bone matrix could be seen in the Col, Col/BMP, and Col/Cs/BMP groups (Fig. 13b-2, c-2, d-2). The results also show that no ectopic bone formation was observed in any of the groups. Importantly, the boundary between host bone and new bone disappeared 8 weeks after implantation (Fig. 13d-2), indicating that osseointegration had been basically completed[31].

The biomechanical properties of an implant are key parameters affecting osseointegration after surgical implantation. In biomechanics, the maximum pull-out force [32, 33] is often used to mechanically evaluate the bone bonding strength between the bone and the implant. In this study, the pull-out test results (Fig. 14) revealed that the pull-out force increased over time for all groups. Col coating on the implant resulted in a greater bonding strength between the implant and the bone (53.09 N at 4 weeks and 74.89 N at 8 weeks) compared to the Ti group (45.80 N at 4 weeks and 74.89 N at 8 weeks). When rhBMP-2 was incorporated into the coatings, the pull-out force increased (63.13 N at 4 weeks and 85.13 N at 8 weeks), while enhanced rhBMP-2 loading resulted in the coating with the highest pull-out strength(89.67N at 4 weeks and 107.01N at 8 weeks). This increase of pull-out strength in comparison with the Ti control group (48.92% increase at 4 weeks and 30.16% increase at 8 weeks) indicates a significant effective improvement in osseointegration compared with previous work[34].

4 Discussion

Since the BMP loading in the coatings was obviously increased, there is no doubt that the chitosan nanospheres played a significant role. The presence of rhBMP-2 appears to accelerate new bone formation and enhance the osseointegration process, but an appropriate concentration of rhBMP-2 is required. The total release of rhBMP-2 should not be lower than 596 ng/cm^2, otherwise osseointegration could not be essentially completed after implantation for 12 weeks [35]. However, the release amount cannot be too great due to the risk of inducing ectopic bone formation. In addition, an effective release period is also required, and it is necessary for the loading material to be able to extend the release period to over 30 days *in vitro*[14] to guarantee the establishment of essential osseointegration within an expected period (3 months) after implantation[36]. However, it is a challenge to load a thin porous coating with a desired amount of rhBMP-2, which must also exhibit appropriate release behavior as before mentioned. Here, we attempted to utilize rhBMP-2-boundchitosannanospheres to modify the microstructures of the porous thin coating, to realize both elevated rhBMP-2 loading and improved release behavior.

After incorporation of chitosan nanospheres into the coatings, the microstructure of the Col/Cs/BMP coating revealed that the nanospheres were present on the pore walls of the coating material (Fig. 1b), and the cross-section morphology was found to have become denser (Fig. 1b-1). In addition, the incorporation

process had almost no influence on the mineral phase in the coatings (Fig. 2). In the modified microstructure, more rhBMP-2 was expected to load due to the increased affinity of its chitosan nanospheres, and the release behavior was expected to improve due to the increase in the diffusion path because of the more tortuous porosity of the coating. In this study, the incorporation process caused the loaded amount of rhBMP-2 of the Col/Cs/BMP coating to reach 1,186 ng/cm^2, a significant increase of 2.7-fold (Fig. 3) in comparison with the Col/BMP coating, and 70% of the total release was postponed from 15 days to 20 days as a result of the injection of chitosan nanospheres (Fig. 4). The reason of drastic increase in the BMP release from Col/Cs/BMP coating around 12 days may be attributed to the decomposition of chitosan nanospheres. Kinetic analysis (Fig. 5) of the release behaviors further proved that the modified microstructure is able to regulate rhBMP-2 release, depressing initial burst-release and improving sustained release. The high rhBMP-2 loading and reasonably sustained release behavior indicate that the present method is an effective way of modifying a porous thin coating, causing it to release rhBMP-2 in the desired manner and thus promote bone formation.

The incorporation of chitosan nanospheres resulted in changes in morphology and chemical composition of the coatings, but these changes had no obvious effects on the adhesion (Fig. 6), proliferation (Fig. 6 and Fig. 7) ormorphology (Fig. 7 and Fig. 8) of the MC3T3-E1 cells cultured on the coatings, and retained the good biocompatibilities of mineralized collagen coatings.

The essential function of rhBMP-2 is to promote osteogenic differentiation. When expression of ALP [4] was used as a marker of osteoblastic differentiation, the MC3T3-E1cells cultured for 7 days on the coatings showed an obvious rhBMP-2 dose-dependent increase, and the level remained high at 14 days for cells cultured on the Col/Cs/BMP coating (Fig. 9). mRNA expression of the osseointegration-related genes osteocalcin (OC) and collagen type I (Col I) are often used as indicators of osteogenic differentiation at the molecular level. The OC and Col I expression of the cells cultured on the coatings also increased as the loading amount of rhBMP-2 was increased for both 7- and 14-day culture (Fig. 10).When cell mineralization level was used as a late stage indicator of osteogenic differentiation[24], the number of nodules, as well as the amount of Alizarin red staining and EDS calcium mapping (Fig. 11) of 21-day cultured cells all demonstrated a remarkable rhBMP-2 dose-dependent increase, with cells cultured on the Col/Cs/BMP coating showed the highest mineralization level. These *in vitro* results indicate that enhanced rhBMP-2 loading (1,186 ng/cm^2) in the Col/Cs/BMP coating can preserve its essential function of promoting the osteogenic differentiation process at different stages.

The aim of incorporating rhBMP-2 is to accelerate new bone formation. In *in vivo* tests, the quantity of new bone formed (Fig. 12 and Fig. 13) was found to significantly increase with increasing rhBMP-2 loading. The boundary between host bone and new bone disappeared by 8 weeks after implantation (Fig. 13 d-2) in the Col/Cs/BMP group, indicating that the implant had basically become integrated with the host bone. Here, the coating was biodegradable and finally the coating would be biologically transformed into the new bone. The results of pull-out tests (Fig. 14) showed that the degree of osseointegration was enhanced dramatically with rhBMP-2 loading, with the increase in pull-out strength being greater after 4-week implantation than that after 8 weeks. This implies that the incorporation of chitosan nanospheres with rhBMP-2 could make a significant contribution to early bone formation (4 weeks), and that this plays an important role in shortening the osseointegration process to almost 8 weeks. The new bone growth would be extremely limited after the completion of osseointegration process as the space for tissue growing around coating was very limited. The BMP loading dependent increase in the pull-out strength could imply that the BMP released from coating played the key role in osseointegration. The Col/Cs/BMP coating group demonstrates good ability to induce bone formation at its surface.

Based on the results from both *in vitro* and *in vivo* tests, the enhanced amount of loaded rhBMP-2 of 1,186 ng/cm^2 in the Col/Cs/BMP coating not only shows the highest loading value in this work, but also demonstrates that it is necessary to reach a desired value range in order to significantly accelerate the osseointegration process, which is essential to shorten recovery time after implantation surgeries.

5 Conclusion

In this study, we show that rhBMP-2 can be incorporated into a porous thin mineralized collagen coating by the electrophoretic injection method, and that enhanced rhBMP-2 loading can be obtained with the aid of chitosan nanospheres. The resulting coating is shown to have a microstructure of chitosan nanospheres tightly adhering to the pore walls of the mineralized collagen coating. The good affinity of chitosan nanospheres for

rhBMP-2 is mainly responsible for the enhanced rhBMP-2 loading, and the change in microstructure causes an improvement in rhBMP-2 release behavior. The enhanced rhBMP-2 loading in this study was able to reach 1,186 ng/cm^2, and resulted in significant increases in proliferation, differentiation and mineralization levels of cultured MC3T3-E1 cells in *in vitro* assays. The enhanced loading also intensified bone density at the bone–implant interface and increased osseointegration in *in vivo* tests, leading to a basic establishment of osseointegration after implantation for 8 weeks, and at the same time this loading amount didn't exceed the upper limit. Hence, the enhanced rhBMP-2 loading is considered to reach a desirable value range, enabling it to significantly accelerate bone tissue growth. This method could be an effective route to significantly increase biological factor loading of porous thin bioactive coatings on metal implants.

Acknowledgements

This work is financially supported by the National Basic Research Program of China (973 Program, 2012CB933600) and by the National Natural Science Foundation of China (51272228, 51072178, 81071258, 81171003, 81271955). Support was also received from the Qianjiang Talent Project of Zhejiang Province (2011R10057) and the research fund of the Science and Technology Department of Zhejiang Province of China (2010C33088).

Notes and references

1. S. B. Goodman, Z. Yao, M. Keeney and F. Yang, *Biomaterials*, 2013, 34, 3174-3183.
2. H. Schliephake and D. Scharnweber, *Journal of Materials Chemistry*, 2008, 18, 2404.
3. A. Fukuda, M. Takemoto, T. Saito, S. Fujibayashi, M. Neo, S. Yamaguchi, T. Kizuki, T. Matsushita, M. Niinomi, T. Kokubo and T. Nakamura, *Acta biomaterialia*, 2011, 7, 1379-1386.
4. Y. Hu, K. Cai, Z. Luo, Y. Zhang, L. Li, M. Lai, Y. Hou, Y. Huang, J. Li, X. Ding, B. Zhang and K. L. Sung, *Biomaterials*, 2012, 33, 3515-3528.
5. H. Wang, N. Eliaz, Z. Xiang, H. P. Hsu, M. Spector and L. W. Hobbs, *Biomaterials*, 2006, 27, 4192-4203.
6. Y. J. Lee, J. S. Ko and H. M. Kim, *Biomaterials*, 2006, 27, 3738-3744.
7. T. Crouzier, F. Sailhan, P. Becquart, R. Guillot, D. Logeart-Avramoglou and C. Picart, *Biomaterials*, 2011, 32, 7543-7554.
8. E. Piek, L. S. Sleumer, E. P. van Someren, L. Heuver, J. R. de Haan, I. de Grijs, C. Gilissen, J. M. Hendriks, R. I. van Ravestein-van Os, S. Bauerschmidt, K. J. Dechering and E. J. van Zoelen, *Bone*, 2010, 46, 613-627.
9. N. M. Moore, N. J. Lin, N. D. Gallant and M. L. Becker, *Acta biomaterialia*, 2011, 7, 2091-2100.
10. Y. Liu, K. de Groot and E. B. Hunziker, *Bone*, 2005, 36, 745-757.
11. Y. Liu, L. Enggist, A. F. Kuffer, D. Buser and E. B. Hunziker, *Biomaterials*, 2007, 28, 2677-2686.
12. P. Q. Ruhe, O. C. Boerman, F. G. Russel, A. G. Mikos, P. H. Spauwen and J. A. Jansen, *Journal of materials science. Materials in medicine*, 2006, 17, 919-927.
13. D. H. Kempen, L. Lu, T. E. Hefferan, L. B. Creemers, A. Maran, K. L. Classic, W. J. Dhert and M. J. Yaszemski, *Biomaterials*, 2008, 29, 3245-3252.
14. S. E. Bae, J. Choi, Y. K. Joung, K. Park and D. K. Han, *Journal of Control Release*, 2012, 160, 676-684.
15. Y. Hu, K. Cai, Z. Luo, D. Xu, D. Xie, Y. Huang, W. Yang and P. Liu, *Acta Biomater*, 2012, 8, 439-448.
16. J. Tu, M. Yu, Y. Lu, K. Cheng, W. Weng, J. Lin, H. Wang, P. Du and G. Han, *J Mater Sci Mater Med*, 2012, 23, 2413-2423.
17. Z. Kong, M. Yu, K. Cheng, W. Weng, H. Wang, J. Lin, P. Du and G. Han, *Colloids and surfaces. B, Biointerfaces*, 2013, 111C, 536-541.
18. Q. Zhang, Q. F. He, T. H. Zhang, X. L. Yu, Q. Liu and F. L. Deng, *Biomed Mater*, 2012, 7, 045002.
19. M. Rinaudo, *Progress in Polymer Science*, 2006, 31, 603-632.
20. S. A. Agnihotri, N. N. Mallikarjuna and T. M. Aminabhavi, *Journal of controlled release : official journal of the Controlled Release Society*, 2004, 100, 5-28.
21. U. Brohede, J. Forsgren, S. Roos, A. Mihranyan, H.

Engqvist and M. Stromme, *Journal of Materials Science - Materials in Medicine* 2009, 20, 1859-1867.

22. P. Yilgor, K. Tuzlakoglu, R. L. Reis, N. Hasirci and V. Hasirci, *Biomaterials*, 2009, 30, 3551-3559.

23. L. L. Lao, N. A. Peppas, F. Y. Boey and S. S. Venkatraman, *International Journal of Pharmaceutics*, 2011, 418, 28-41.

24. J. Park, S. Bauer, K. A. Schlegel, F. W. Neukam, K. von der Mark and P. Schmuki, *Small*, 2009, 5, 666-671.

25. M. Kushwaha, X. Pan, J. A. Holloway and I. L. Denry, *Dental materials : official publication of the Academy of Dental Materials*, 2012, 28, 252-260.

26. H. T., *Journal of Pharmaceutical Sciences*, 1963, 52, 1145-1149.

27. L. Sun, L. Wu, C. Bao, C. Fu, X. Wang, J. Yao, X. Zhang and B. C. Van *Materials Science and Engineering: C*, 2009, 29, 1829-1834.

28. T. Yonezawa, J. W. Lee, A. Hibino, M. Asai, H. Hojo, B. Y. Cha, T. Teruya, K. Nagai, U. I. Chung, K. Yagasaki and J. T. Woo, *Biochem Biophys Res Commun*, 2011, 409, 260-265.

29. G. Tan, L. Zhou, C. Ning, Y. Tan, G. Ni, J. Liao, P. Yu and X. Chen, *Applied Surface Science*, 2013, 279, 293-299.

30. K. E. H. Alireza Rezania, *Journal of Biomedical Materials Research*, 2000, 52, 595-600.

31. H. Aita, N. Hori, M. Takeuchi, T. Suzuki, M. Yamada, M. Anpo and T. Ogawa, *Biomaterials*, 2009, 30, 1015-1025.

32. X. Liu, S. Wu, K. W. Yeung, Y. L. Chan, T. Hu, Z. Xu, J. C. Chung, K. M. Cheung and P. K. Chu, *Biomaterials*, 2011, 32, 330-338.

33. S. S. Huja, A. S. Litsky, F. M. Beck, K. A. Johnson and P. E. Larsen, *American journal of orthodontics and dentofacial orthopedics : official publication of the American Association of Orthodontists, its constituent societies, and the American Board of Orthodont*, 2005, 127, 307-313.

34. M. Monjo, S. F. Lamolle, S. P. Lyngstadaas, H. J. Ronold and J. E. Ellingsen, *Biomaterials*, 2008, 29, 3771-3780.

35. J. Becker, A. Kirsch, F. Schwarz, M. Chatzinikolaidou, D. Rothamel, V. Lekovic, M. Laub and H. P. Jennissen, *Clinical oral investigations*, 2006, 10, 217-224.

36. Z. Li, X. Gu, S. Lou and Y. Zheng, *Biomaterials*, 2008, 29, 1329-1344.

Figures

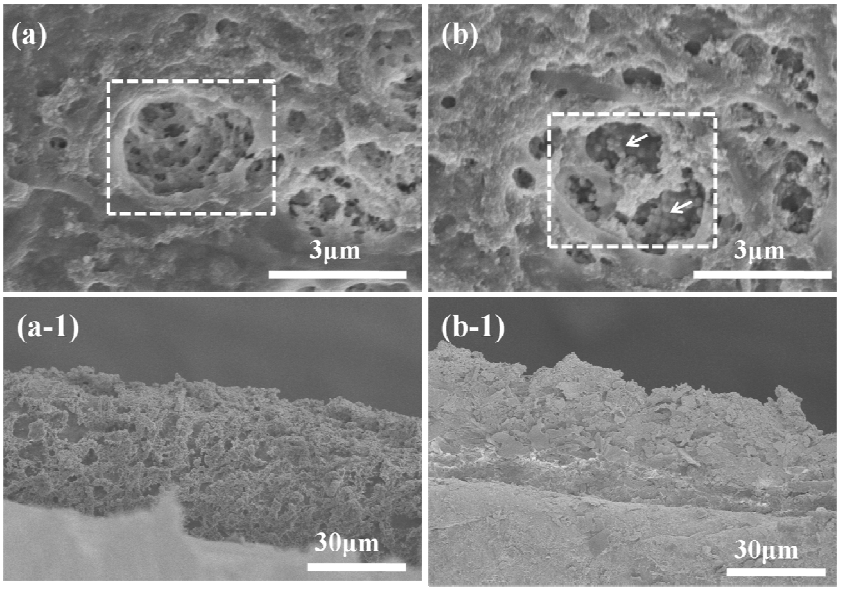

Fig. 1 SEM images of the coatings:(a) Surface morphology of Col/BMP coating (a-1) Cross section morphology of Col/BMP coating (b) Surface morphology of Col/Cs/BMP coating (b-1) Cross section morphology of Col/Cs/BMP coating. The arrows point to chitosan nanospheres

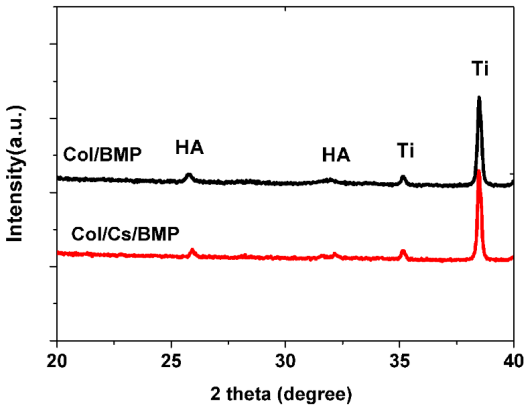

Fig. 2 XRD patterns of different coatings: Col/BMP and Col/Cs/BMP coatings

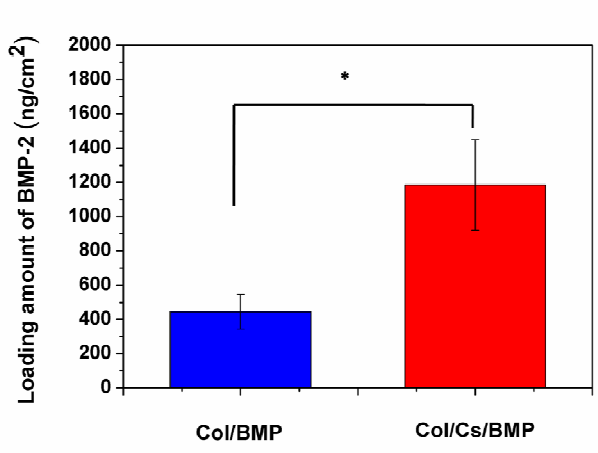

Fig. 3 rhBMP-2 loading amount in Col/BMP and Col/Cs/BMP coatings. Data shown are means ± SD of triplicate assays. Asterisks denote significant differences between different coatings (* $p < 0.05$)

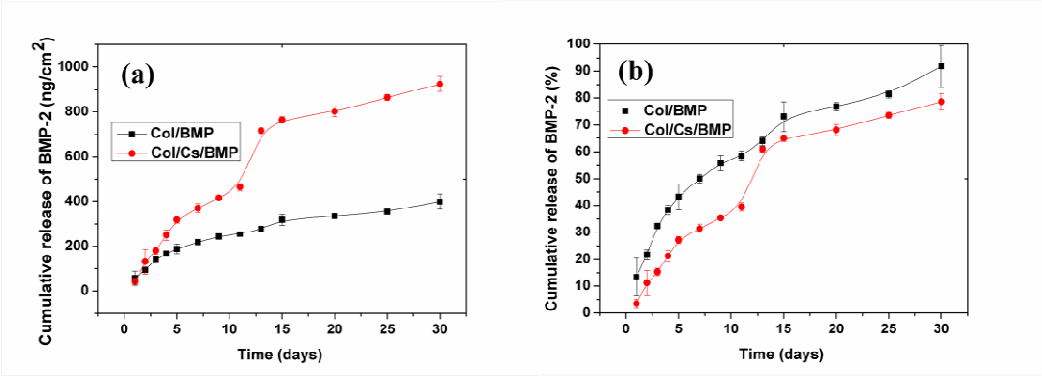

Fig. 4 Cumulative release profile of rhBMP-2 of Col/BMP and Col/Cs/BMP coatings: (a) Release profile (ng/cm^2) of rhBMP-2 from the coatings (b) Release profile (%) of rhBMP-2 from the coatings. Data shown are means ± SD of triplicate assays

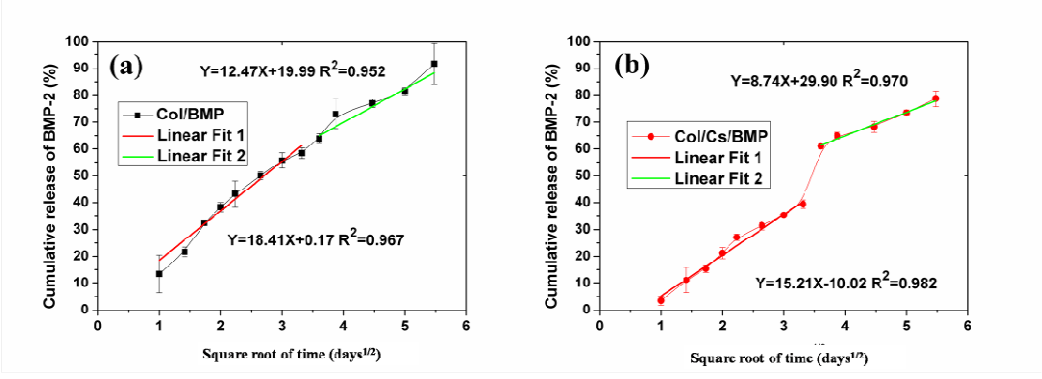

Fig. 5 Linear fit of release curve of (a) Col/BMP coating (b) Col/Cs/BMP coating. Data shown are means ± SD of triplicate assays

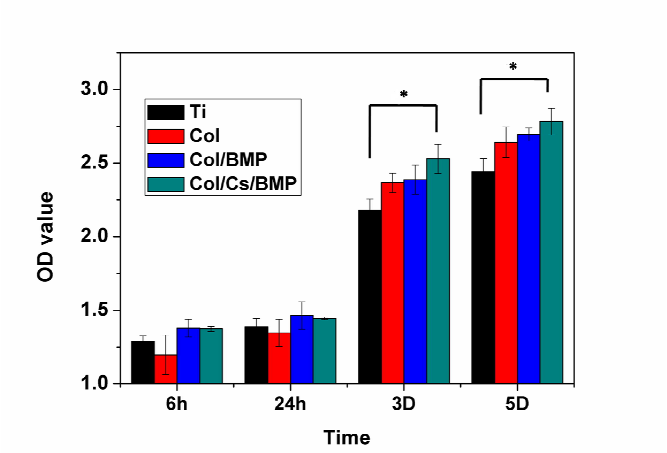

Fig. 6 cck-8 activity of 6h, 24 h, 72 h, 3 day, 5 day of different groups. Data shown are means ± SD of triplicate assays. Asterisks denote significant differences between different groups (* $p < 0.05$)

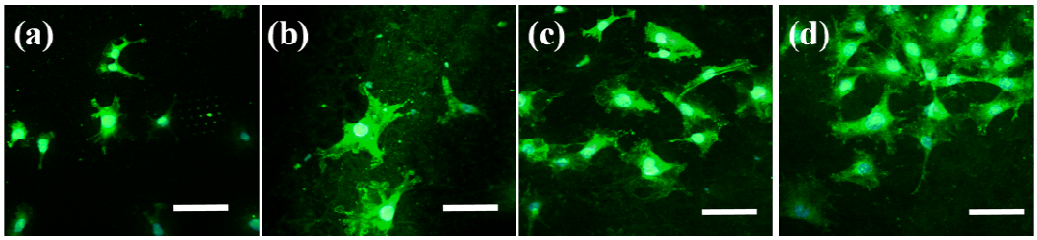

Fig. 7 Representative vinculin fluorescence images of cells on different groups: (a) Ti (b) Col coating (c) Col/BMP coating (d) Col/Cs/BMP coating (the scale bar is 10μm)

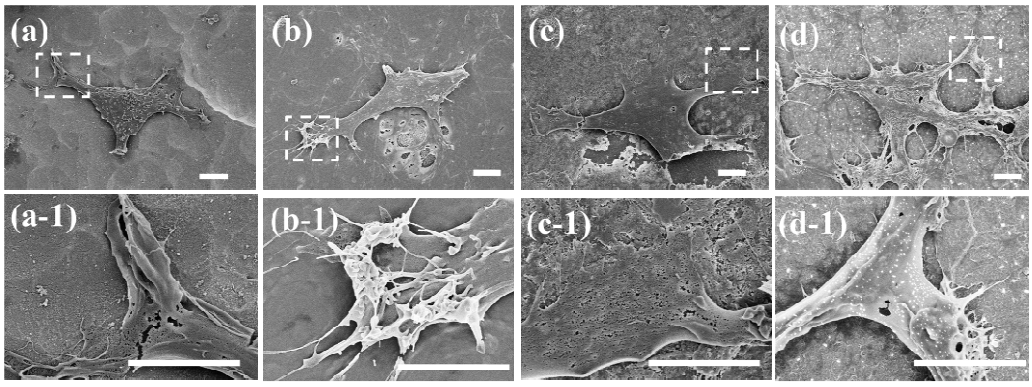

Fig. 8 SEM images of cell morphology on different groups: (a) Ti (b) Col coating (c) Col/BMP coating (d) Col/Cs/BMP coating (the scale bar is 5 μm)

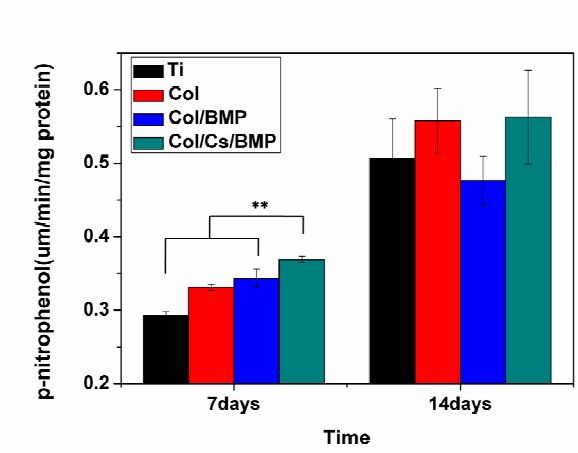

Fig. 9 Alkaline phosphatase expressed level of MC3T3-E1 cells cultured on different groups after culture for 7 days and 14 days, respectively; Data shown are means ± SD of triplicate assays. Asterisks denote significant differences between different groups ($p < 0.01$)**

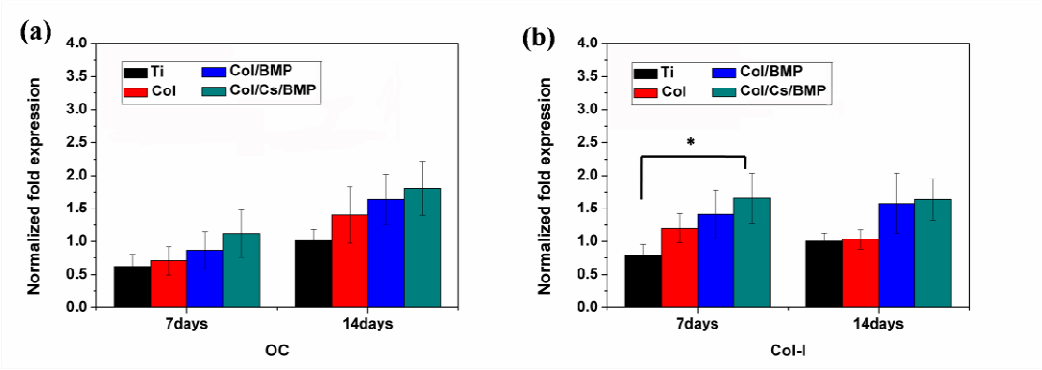

Fig. 10 Relative mRNA expression of different groups:(a)Osteocalcin; (b) Col Ⅰ. The value was normalized to GAPDH. Data shown are means ± SD of triplicate assays. Asterisks denote significant differences between different groups (* $p < 0.05$);

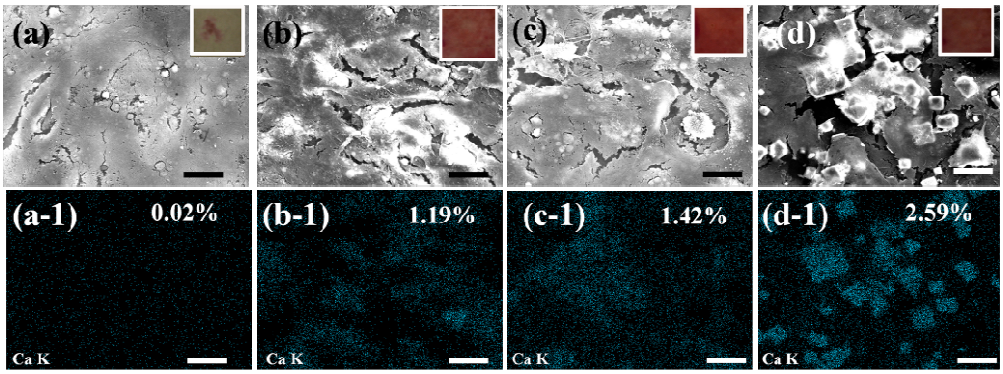

Fig. 11 SEM images and EDS mapping(calcium) of different groups: (a), (a-1) Ti; (b), (b-1) Col coating; (c), (c-1) Col/BMP coating; (d), (d-1) Col/Cs/BMP coating. Insets are samples after Alizarin Red staining .The scale bar is 10 μm.

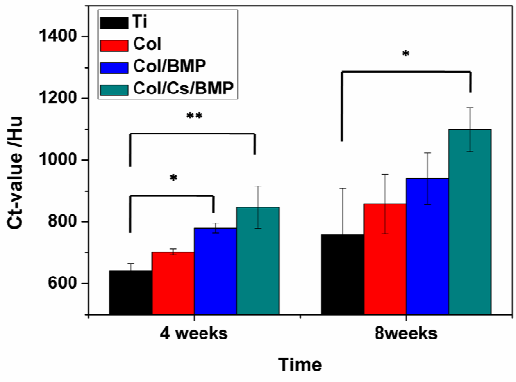

Fig. 12 CT-value of different groups. Data shown are means ± SD of triplicate assays. Asterisks denote significant differences between different groups(* $p < 0.05$, ** $p < 0.01$);

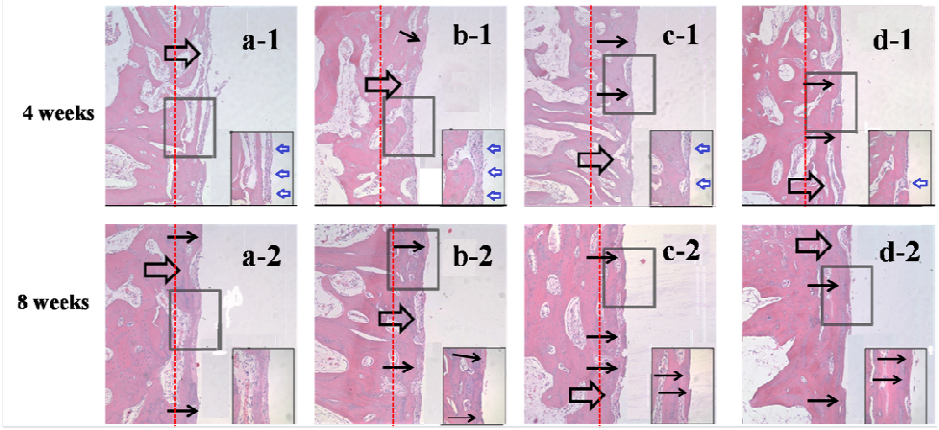

Fig. 13 Histological observations (H&E staining): a: Ti, b: Col, c:Col/BMP, d: Col/Cs/BMP. Large picture:×100, inset picture: ×400. The blank part represented the location of implant. The big arrows point to the fracture of plant pitter. The small black arrows point to the dense bone matrix. The small blue arrows point to the unconnective tissues. The red line represent the boundary of new bone and old bone.

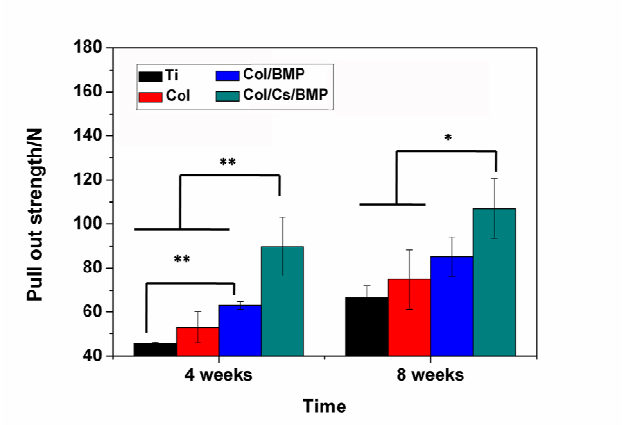

Fig. 14 Pull out strength of different groups after 4 week and 8 week implantation. Data shown are means ± SD of triplicate assays. Asterisks denote significant differences between different groups (* $p < 0.05$, ** $p < 0.01$);

Colour graphic:

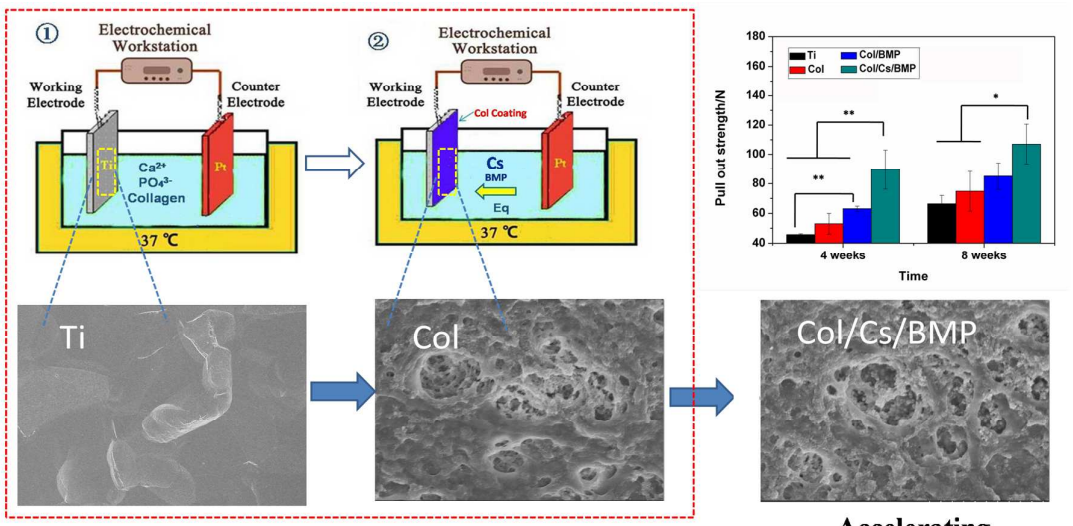

Text:

Osseointegration significantly accelerated by enhanced rhBMP-2 loading in thin mineralized collagen coatings through aid of electrochemically injected chitosan nanospheres